expensive instrumentation can detect the expected changes in stratospheric water vapour. Such measurements at five global locations, for example the sites of the Network for Detection of Stratospheric Change[37], together with future satellite systems, are needed to address the issue of future global changes in stratospheric water vapour associated with methane increases and tropospheric warming. □

Received 16 December 1994; accepted 7 February 1995.

1. Shine, K. P., Derwent, R. G., Wuebbles, D. J. & Morcrette, J.-J. in *Climate Change: The IPCC Scientific Assessment* (eds Houghton, J. T., Jenkins, G. J. & Ephraums, J. J.) 41–68 (Cambridge Univ. Press, 1990).
2. Brassuer, G. P. & Solomon, S. *Aeronomy of the Middle Atmosphere* (Reidel, Dordrecht, 1986).
3. Harries, J. E. *Rev. Geophys. Space Phys.* **14,** 565–575 (1976).
4. *Atmospheric Ozone 1985*, Vol. III, Report No. 16, 951–979 (World Meteorological Organization, Geneva, 1985).
5. Elliott, W. P. & Gaffen, D. J. *Bull. Am. met. Soc.* **72,** 1507–1520 (1991).
6. Garand, L., Grassotti, C., Hallé, J. & Klein, G. L. *Bull. Am. met. Soc.* **73,** 1417–1423 (1992).
7. Jones, R. L. *et al. Q. Jl R. met. Soc.* **112,** 1127–1143 (1986).
8. Rind, D. *et al.*; McCormick, M. P. *et al.*; Chiou, E. W. *et al.*; Larsen, J. C. *et al. J. geophys. Res.* **93,** 4835–4918 (1993).
9. Tuck, A. F., Kelly, K. K., Russell, J. M. III, Harries, J. E. & Webster, C. R. *EOS* **74,** 85 (1993).
10. Kelly, K. K., Tuck, A. F. & Davies, T. *Nature* **353,** 244–247 (1991).
11. Mastenbrook, H. J. & Oltmans, S. J. *J. atmos. Sci.* **40,** 2157–2165 (1983).
12. Hyson, P. *Q. Jl R. met. Soc.* **109,** 285–294 (1983).
13. Cluley, A. P. & Oliver, M. J. *Q. Jl R. met. Soc.* **104,** 511–526 (1978).
14. Blake, D. R. & Rowland, F. S. *Science* **239,** 1129–1131 (1988).
15. Steele, L. P. *et al. Nature* **358,** 313–316 (1992).
16. Folland, C. K., Karl, T. R. & Vinnikov, K. Y. A. in *Climate Change: The IPCC Scientific Assessment* (eds Houghton, J. T., Jenkins, G. J. & Ephraums, J. J.) 194–238 (Cambridge Univ. Press, 1990).
17. Hansen, J. *et al.* in *Climate Processes and Climate Sensitivity* (eds Hansen, J. & Takahashi, T.) 130–163 (Geophys. Mon. Ser. 29, AGU, Washington DC, 1984).
18. Wang, W. C., Yung, Y. L., Lacis, A. A., Mo. T. & Hansen, J. E. *Science* **194,** 685–690 (1976).
19. Hansen, J., Lacis, A. & Prather, M. *J. geophys. Res.* **94,** 16417–16421 (1989).
20. Levy, H. II *Science* **173,** 141–143 (1971).
21. Hofmann, D. J. & Oltmans, S. J. *Geophys. Res. Lett.* **19,** 2211–2214 (1992).
22. Rodriquez, J. M., Ko, M. K. W. & Sze, N. D. *Geophys. Res. Lett.* **15,** 257–260 (1988).
23. Oltmans, S. J. in *Proc. 1985 int. Symp. Moisture and Humidity*, 251–258 (Instrument Society of America, Research Triangle Park, North Carolina, 1985).
24. Goff, J. A. & Gratch, S. *Trans. Am. Soc. Heat and Vent. Engng.* **52,** 95 (1946).
25. Harries, J. E. *et al. J. geophys. Res.* (in the press).
26. Lahoz, W. A. *et al. J. geophys. Res.* (in the press).
27. McCormick, M. P. *et al. J. geophys. Res.* **98,** 4867–4874 (1993).
28. LeTexier, H., Solomon, S. & Garcia, R. R. *Q. Jl R. met. Soc.* **114,** 291–295 (1988).
29. Rasmussen, R. A. & Khalil, M. A. K. *J. geophys. Res.* **89,** 11599–11605 (1984).
30. Dlugokencky, E. J. *et al. J. geophys. Res.* **99,** 17021–17043 (1994).
31. Kley, D. *et al. Geophys. Res. Lett.* **9,** 617–620 (1982).
32. Gutzler, D. S. *Geophys. Res. Lett.* **19,** 1595–1598 (1992).
33. Kelly, K. K. *et al. J. geophys. Res.* **98** 8713–8723 (1993).
34. Danielsen, E. F. *Geophys. Res. Lett.* **9,** 605–608 (1982).
35. Douglas, A. R. *et al. The Atmospheric Effects of Stratospheric Aircraft: A First Program Report* (eds Prather, M. L. & Wesoky, H. L.) 33–61 (NASA Ref. Publ. 1272, 1992).
36. Mastenbrook, H. J. *J. atmos. Sci.* **25,** 299–311 (1968).
37. Kurylo, M. J. & Solomon, S. *Network for the Detection of Stratospheric Change: A Status and Implementation Report* (NASA, Washington DC, 1990).

ACKNOWLEDGEMENTS. We thank F. Polacek III for instrument production and preparation, and balloon launches throughout the measurement programme.

Circulation in the glacial North Atlantic inferred from grain-size measurements

I. N. McCave, B. Manighetti & N. A. S. Beveridge

Department of Earth Sciences, University of Cambridge, Downing Street, Cambridge CB2 3EQ, UK

RECORDS of nutrient proxies in marine sediments indicate that the nutrient distribution—and hence circulation—of the glacial North Atlantic Ocean was markedly different from that of today[1,2]. But these tracers are influenced by several biogeochemical factors unrelated to ocean circulation[3–6], and thus do not provide a direct measure of the vigour of circulation. Distributions of grain size in marine sediments can provide such information, owing to the sorting effects of currents[7,8], if the characteristics of the input sediment flux are known. Here we present a record, inferred from grain-size measurements, of variations in the relative strength of deep and intermediate currents in the eastern North Atlantic over the past 25,000 years. We find that glacial intermediate water flowed rapidly at depths of between 1,100 and 2,000 m. In contrast, deep-water circulation was sluggish during the last glaciation, but increased in strength shortly after the glacial maximum. This would have resulted in increased heat flux to high latitudes, and may have triggered sudden deglaciation. Deep current strengths declined again at the start of termination stage IA and during the Younger Dryas, perhaps as a result of iceberg discharges (the so-called Heinrich events[9,10]). A remarkably similar record of grain-size variations has been found in the western North Atlantic[11], indicating that these changes in circulation are ocean-wide.

The conveyor-belt system of North Atlantic Deep Water produced in the Norwegian and Greenland seas and compensating surface return of the North Atlantic drift exercises an important influence upon regional climate via the transport of heat from low to high latitudes[12]. At present, sub-thermocline waters of the North Atlantic are nutrient-depleted due to the sinking of surface waters to form North Atlantic Deep Water (NADW). However, both carbon isotopes[1,4,13] and Cd/Ca ratios[2] in benthic foraminifera indicate that the glacial water column was highly stratified, with nutrient-depleted intermediate waters at depths shallower than 2,000 m overlying nutrient-enriched waters. This evidence has been interpreted as showing that the glacial North Atlantic was vigorously ventilated at intermediate depths by surface waters sinking in the north[2]. These conclusions are not unequivocal, however, because of changes in the preformed nutrient content of surface water, atmosphere–water CO_2 equilibrium[3] and carbon inventory[4]. There are also questions concerning the reliability of benthic foraminifera as recorders of bottom-water chemistry because of rapid seasonal influx of phytodetritus[5] and dissolution[6].

As an alternative to chemical tracers of water-mass evolution, we employ here a more direct physical proxy of ocean circulation, based on the grain-size characteristics of marine sediments. The mean size of the non-cohesive silt fraction (10–63 μm) is used as an indicator of relative current strength because bottom currents size-sort coarse silt during events of resuspension and ensuing deposition. Stronger currents yield a coarser mean size of the non-cohesive silt fraction, acting through both selective deposition and winnowing[8].

The cores examined in this work are from the UK Biogeochemical Ocean Flux Study (BOFS) sites, between 50–60° N and 15–25° W, and range in depth from 1,100–4,045 m (Fig. 1). Reliable age control was achieved through accelerator mass spectrometry ^{14}C dating of core BOFS 5K, and correlation to the rest of the suite via oxygen- and carbon-isotope profiles, magnetic susceptibility, planktonic foraminiferal species abundance, carbonate content, volcanic ash peaks and X-radiographic characteristics[9,14] (Fig. 2). Grain-size analysis was carried out on the non-carbonate fraction (opal is <1%). Textural parameters have previously been related to bottom-water circulation both in the modern ocean[7] and in palaeoceanographic investigations[11,15,16]. But application of the technique has been limited, largely because of presumed difficulties with unknown source functions[17]. The glacial northeast Atlantic received variable input of ice-rafted detritus, which might cause changes in mean grain size independent of variation in bottom currents. We approach this problem by identifying the characteristics of the input flux as a function of time at a site which is unaffected by current winnowing or focusing. Grain-size changes in sortable silt from current-affected sites are calculated by difference from the input flux time-series (Fig. 2). The resulting variation in differential grain size is attributed to fluctuating current speed. To define the input flux, we use core BOFS 6K from the East Thulean rise which is away from the path of major currents and separated from the Rockall plateau by the South Rockall gap

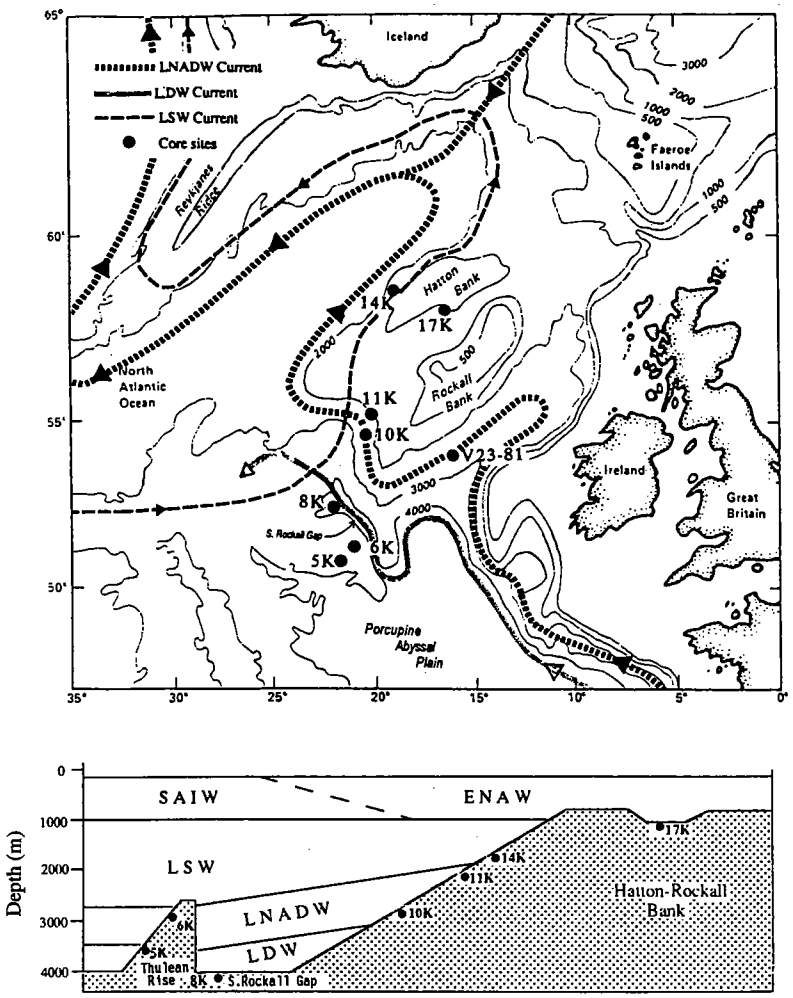

FIG. 1 Top, location of BOFS core sites and core V23-81[20]. The paths of major deep-water currents are shown as dashed and dotted lines. Bottom, schematic cross-section (approximately south–north) illustrating present-day water-mass distribution in the Rockall area. These water masses are: the Lower Deep Water (LDW) of McCartney[18], a derivative of Antarctic Bottom Water (AABW) which is warmer than AABW but which has higher Si and nutrient content than northern source water. Above this lies the familiar sequence of lower North Atlantic Deep Water (LNADW), Labrador Sea Water (LSW or upper North Atlantic Deep Water, UNADW), and shallower volumetrically insignificant intermediate waters (Sub-Arctic Intermediate Water and Eastern North Atlantic Water, SAIW and ENAW, respectively)[19]. Indicated flow paths are taken from McCave and Tucholke[30] and McCartney[18].

(Fig. 1). The input flux at BOFS 6K shows a fairly constant low mean grain size during the glacial period and early deglaciation, rising by ~3 μm during termination IB (Fig. 2*a*).

Cores from BOFS sites 8K and 10K are at depths of 4,045 m (under Lower Deep Water[18], LDW) and 2,777 m (under lower North Atlantic Deep Water[19], LNADW), respectively, on sediment drifts (Fig. 1) and have the potential to monitor changes in the strength of deep-water currents. Values of differential grain size for these cores are markedly similar, and reveal significant downcore variation, implying past fluctuations in current strength (Fig. 2*b*, *c*). Covariation of the silt mean records from present-day LDW- and LNADW-influenced sites suggests either a strong link between the speed of the two water masses or movement of the boundary between them so that both sites were bathed by the same water. Chemical data suggest that the top surface of the LDW was at ~2,000 m depth in this area during the last glacial[20,21], putting both sites under glacial LDW.

The flow of glacial LDW was sluggish at site 8K during the glacial period. The area is so far from the Antarctic Bottom Water (AABW) source that it is not possible to make inferences about the southern source strength from our data. However, data from regions closer to the AABW source suggest slower flow during the glacial than at present[15,22]. Our records from both core 8K and 10K indicate a marked increase in flow speed between the glacial maximum and the onset of deglaciation, peaking at 15–16 kyr ago. The record of grain-size variation on the Blake outer ridge in the western North Atlantic, is remarkably similar[11] (Fig. 2*e*), suggesting that the event is of ocean-wide significance.

Core V23-81 from ~2,400 m depth in the Rockall region (Fig. 1) shows a maximum in $\delta^{13}C$ coincident in time with the inferred pulse in deep current speed before termination IA (Fig. 2*d*)[20]. This suggests an increase in the input of nutrient-depleted water of northern source. The inferred increase in the flux (product of thickness and speed) of northern source water through South Rockall gap could have been caused by increased production rate as speed at site 10K increased. The increase in LDW flow speed occurred because the two water masses are linked in geostrophic flow to the west through South Rockall gap[23,24]. In the western basin, glacial intermediate water extended down to 2,500 m depth, but present-day NADW goes down to ~4,300 m (refs 2, 11). It is possible that the region below 3,000 m on Blake outer ridge was also still under glacial LDW at this time, but alternatively at least the shallower Blake outer ridge stations may have directly recorded the LNADW pulse. On Blake outer ridge, the present LDW and NADW both flow to the south[25]. The deep gyres of the western basin are partly driven by Gulf Stream thickness variations[26], and an increase in Gulf Stream flux may have driven a more vigorous deep circulation of both glacial LDW and LNADW. An increase in the Gulf Stream flux would also have contributed the source water which cooled north of the late glacial polar front, probably in the Norwegian Sea, yielding the pre-termination pulse of deep water. The significance of this higher-speed pulse is that the surface waters which fed it would have contributed heat to northern regions and possibly have been the trigger for the deglaciation which immediately followed it, starting in the Nordic area[27]. At this time insolation was increasing in the Northern Hemisphere but decreasing in the south, yet there was a brief period of marked retreat of mountain glaciers in the Andes and New Zealand just before termination IA[12], coinciding with the pulse in LNADW current speed shown here. Control by deep circulation may well be involved.

After the start of termination IA, inferred flow speeds at sites 8K and 10K abruptly decreased and reached a minimum between 13 and 14 kyr. A pronounced minimum in $\delta^{13}C$ values at 13–14 kyr (during the deglaciation) in core V23-81 suggests reduced influence of northern source water. This abrupt decline is coincident with Heinrich ice-rafting event 1 (refs 9, 10), which introduced fresh water to the surface ocean through iceberg melting, decreasing the density of surface water by an amount probably sufficient to cause cessation of deep convection. Following this event, both differential grain size and $\delta^{13}C$ value increased, indicating a return to more vigorous deep-water circulation during the Allerod warming (~12 kyr ago). Current vigour apparently declined temporarily at the start of the Younger Dryas at the depth of core 10K, and this is matched by a minimum in $\delta^{13}C$ values in V23-81, again perhaps caused by a buoyant meltwater cap[28].

At shallower depths, differential grain sizes in cores BOFS 11K (2,004 m), 14K (1,756 m) and 17K (1,100 m) demonstrate faster current speeds in the glacial and Younger Dryas than in

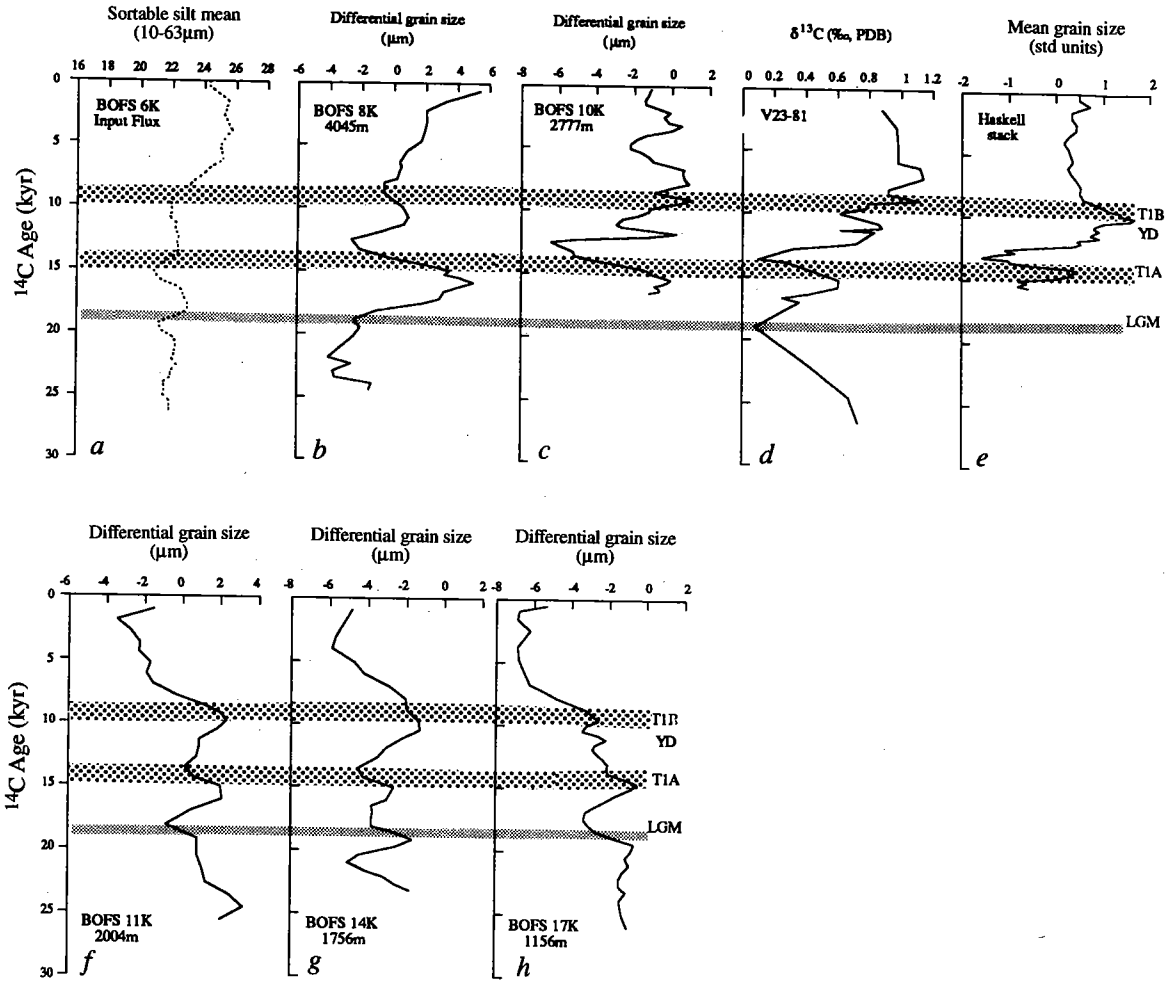

FIG. 2 Grain-size and carbon-isotope records in North Atlantic cores. Ages are ^{14}C (Libby) years, corrected for the reservoir effect by subtracting 400 years. The position of terminations IA and IB (TIA and TIB) are shaded, and the Younger Dryas (YD) and Last Glacial Maximum (LGM) are also indicated. *a*, 10–63 μm non-carbonate silt mean size as a function of time in core BOFS 6K, representing the input flux unmodified by current activity. The profile is smoothed with a three-point moving average. *b*, *c*, 10–63 μm silt mean grain size in BOFS cores 8K (*b*) and 10K (*c*), expressed as difference from the input flux in core 6K (differential grain size). *d*, Benthic $\delta^{13}C$ record (*Cibicidoides wuellerstorfi*) in Core V23-81[20]. *e*, Weighted-average mean grain size (in units of standard deviation about the mean) of 6–63 μm non-carbonate silt in cores CH88-7P, 10P and 11P[9] from the Blake outer ridge (30° N, 74° W), for which age control is achieved by correlation with core KN31-GPC-5[31]. *f–h*, Differential grain size (as defined for *b* and *c*) of the 10–63 μm silt in intermediate-depth cores BOFS 11K, 14K and 17K. (Some of the data on which the correlations are based is in ref. 9 (magnetic susceptibility and $\delta^{18}O$ *Bulloides* for some cores) but all data may be obtained from the authors on request. Note that many of these data are on the BOFS database on CD-ROM from the British Oceanographic Data Centre, Proudman Lab., Bidston, Merseyside.)

the Holocene. This is consistent with carbon-isotope and Cd/Ca data, which indicate nutrient-depleted glacial waters at these depths[2,21]. Covariation of grain-size records in these cores implies that all three sites were subject to the same flow regime during the glacial period. There is also a pronounced decline in speed at all three sites during the Holocene (from a high just before termination IB at 11K, 14K and Blake outer ridge) (Fig. 2*e–h*).

These grain-size records provide direct evidence for changes in the vigour of palaeocirculation which is independent of isotopic and chemical indicators. Temporal patterns of circulation reassuringly similar to some of those inferred from isotopic and chemical tracers are demonstrated. At a time when the reliability of benthic geochemical data is in question[5,29], our method provides direct information on the physical oceanographic changes driving geochemical variation. □

Received 27 June 1994; accepted 30 January 1995.

1. Duplessy, J C. *et al. Paleoceanography* **3,** 343–360 (1988).
2. Boyle, E. A. & Keigwin, L. *Nature* **330,** 35–40 (1987).
3. Lynch-Stieglitz, J. & Fairbanks, R. G. *Nature* **369,** 308–310 (1994).
4. Oppo, D. & Fairbanks, R. G. *Earth planet. Sci. Lett.* **86,** 1–15 (1987).
5. Mackensen, A., Hubberten, H-W., Bickert, T., Fischer, G. & Fütterer, D. K. *Paleoceanography* **6,** 587–610 (1993).
6. McCorkle, D. C., Martin, P. A., Lea, D. W. & Klinkhammer, G. P. (abstr.) *Eos* **75,** 54 (1994).
7. Ledbetter, M. T. *Nature* **321,** 423–425 (1986).
8. McCave, I. N., Manighetti, B. & Robinson, S. G. *Paleoceanography* (in the press).
9. Manighetti, B., Maslin, M. A., McCave, I. N. & Shackleton, N. J. *Paleoceanography* (in the press).
10. Bond, G. *et al. Nature* **360,** 245–249 (1992).
11. Haskell, B. J., Johnson, T. C. & Showers, W. J. *Paleoceanography* **6,** 21–31 (1991).
12. Broecker, W. S. & Denton, G. H. *Geochim. cosmochim. Acta.* **53,** 2465–2501 (1989).
13. Curry, W. B., Duplessy, J. C., Labeyrie, L. D. & Shackleton, N. J. *Paleoceanography* **3,** 317–341 (1988).
14. Manighetti, B. thesis, Univ. Cambridge (1993).
15. Ledbetter, M. R. *Mar. Geol.* **58,** 137–149 (1984).
16. Wang, H. & McCave, I. N. *J. geol. Soc. Lond.* **147,** 373–383 (1990).
17. Corliss, B. H., Martinson, D. G. & Keffer, T. *Bull. Geol. Soc. Am.* **97,** 1106–1121 (1986).
18. McCartney, M. S. *Progr. Oceanogr.* **29,** 283–384 (1992).
19. Harvey, J. G. *Deep-Sea Res.* **29,** 1021–1033 (1982).
20. Jansen, E. & Veum, T. *Nature* **343,** 612–614 (1990).
21. Oppo, D. W. & Lehman, S. J. *Science* **259,** 1148–1152 (1993).
22. Pudsey, C. J. *Mar. Geol.* **107,** 9–33 (1992).
23. Schmitz, W. J. & McCartney, M. S. *Rev. Geophys.* **31,** 29–49 (1993).
24. Dickson, R. R. & Brown, J. *J. geophys. Res.* **99,** 12328–12342 (1994).
25. Amos, A. F., Gordon, A. L. & Schneider, E. D. *Deep-Sea Res.* **18,** 145–165 (1971).
26. Hogg, N. G. & Stommel, H. *Deep-Sea Res.* **32,** 1181–1193 (1985).
27. Jones, G. A. & Keigwin, L. D. *Nature* **336,** 56–59 (1988).

28. Bond, G. *et al. Nature* **365,** 143–147 (1993).
29. Boyle, E. A. *A. Rev. Earth planet. Sci.* **20,** 245–287 (1992).
30. McCave, I. N. & Tucholke, B. E. in *The Western North Atlantic Region* Vol. M (eds Vogt, P. R. & Tucholke, B. E.) 451–468 (Geol. Soc. Am. Boulder, 1986).
31. Keigwin, L. D. & Jones, G. A. *Deep-Sea Res.* **36,** 845–867 (1989).

ACKNOWLEDGEMENTS. We thank G. Foreman and M. Hall for technical assistance, B. Haskell for data and N. Shackleton for encouragement. This work was supported by the UK NERC for BOFS.

Continental crust composition constrained by measurements of crustal Poisson's ratio

George Zandt* & Charles J. Ammon†

* Institute of Geophysics and Planetary Physics, Lawrence Livermore National Laboratory, 7000 East Avenue, L-202, Livermore, California 94550, USA
† Department of Earth and Atmospheric Sciences, Saint Louis University, 3507 Laclede Avenue, Saint Louis, Missouri 63103, USA

DECIPHERING the geological evolution of the Earth's continental crust requires knowledge of its bulk composition and global variability. The main uncertainties are associated with the composition of the lower crust. Seismic measurements probe the elastic properties of the crust at depth, from which composition can be inferred. Of particular note is Poisson's ratio, σ; this elastic parameter can be determined uniquely from the ratio of P- to S-wave seismic velocity, and provides a better diagnostic of crustal composition than either P- or S-wave velocity alone[1]. Previous attempts to measure σ have been limited by difficulties in obtaining coincident P- and S-wave data sampling the entire crust[2]. Here we report 76 new estimates of crustal σ spanning all of the continents except Antarctica. We find that, on average, σ increases with the age of the crust. Our results strongly support the presence of a mafic lower crust beneath cratons, and suggest either a uniformitarian craton formation process involving delamination of the lower crust during continental collisions, followed by magmatic underplating, or a model in which crust formation processes have changed since the Precambrian era.

Estimates of the bulk composition of the Earth's crust are limited by the uncertainty in the composition of the lower crust. A variety of approaches, including seismic, crustal xenolith and isotopic studies, as well as direct examination of exposed crustal sections, have led to various estimates of lower-crustal compositions ranging from felsic to mafic[2–5]. Seismic measurements, perhaps the most direct method for probing the lower crust, have been impeded by the non-uniqueness of compressional-wave velocities (v_P) for the lower crust where both higher metamorphic grade and increasing mafic content can have similar effects[2] on v_P. The non-uniqueness is partially alleviated by the addition of shear-wave (v_S) data to estimate v_P/v_S (ref. 1), and hence Poisson's ratio, σ. For common rock types, σ varies from 0.20 to 0.35 and is particularly sensitive to composition; increasing the silica content lowers σ and high mafic content increases it (ref. 6). For lower-crustal rocks, low σ (<0.26), intermediate σ (0.26–0.28) and high σ (>0.28) are characteristic of felsic, intermediate and mafic compositions, respectively[2]. Although the importance of σ has been recognized for at least two decades[1], a comprehensive, 1992 review paper[2] cited only 11 reliable *in situ* measurements of Poisson's ratio. We use a simple teleseismic method, and data from the growing global network of digital broadband seismograph stations, to increase the number of estimates of Poisson's ratio by a factor of seven.

We measure the travel times of converted waves in the P waveforms of a teleseism recorded at a single seismic station to estimate the v_P/v_S of the crust beneath the site. A teleseismic P-wave incident on the base of the crust generates a converted S-wave (Ps) and a converted P-wave multiple (PpPms) within the crust[7] (Fig. 1). The converted phases are isolated from source effects by deconvolving the vertical from the radial component of the P waveform to produce a time series called a receiver function[8–10]. The ratio of the Ps–P time and the PpPms–Ps time is directly related to v_P/v_S, independent of crustal thickness but with a slight dependence[11] on v_P; for a range in v_P of 6.0–6.75 km s^{-1}, the change in v_P/v_S is at most 0.05 and the change in σ is no more than 0.02. Our approach is similar in principle to another single-station teleseismic technique[12]. This other method uses the redundancy of multiple phases within one seismogram, but our method does not require computation of synthetic seismograms so making it suitable for a rapid global survey. As a test of our methodology, we compared our measurements with those from a coincident seismic refraction study. Both compressional- and shear-wave Moho reflections were recorded in a recent seismic refraction experiment in eastern Ontario and northern New York state[13]. The ratio of the S-wave and P-wave travel times indicates a Poisson's ratio of 0.28 ± 0.01 for the crust in the southeastern Precambrian Grenville province[14]. We

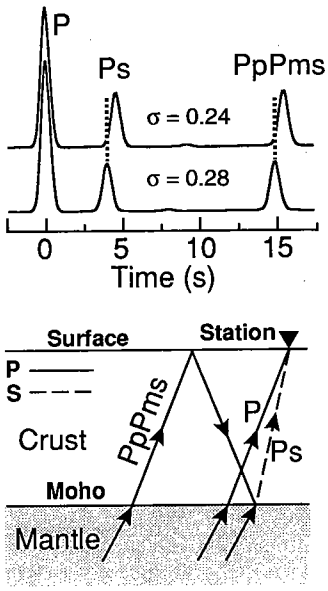

FIG. 1 Bottom, geometry of ray paths for the P wave, the converted wave Ps, and multiple converted wave PpPms generated by a teleseismic plane wave interacting with the impedance contrast at the base of the crust. Top, synthetic receiver functions for a crust with Poisson's ratio of 0.24 (upper trace) and 0.28 (lower trace). We calculate v_P/v_S (then σ) from the ratio of differential times (Ps–P)/(PpPms–Ps) and estimate the crustal thickness using the Ps–P time and the estimated value of v_P/v_S for a range of average crustal P-wave velocities. The main assumption in this method is that the Ps and PpPms phases propagate in a laterally uniform crust over the distance sampled by the phases (20–50 km). A tangential receiver function is non-zero only in the presence of lateral heterogeneity and is used to assess the quality of measurements made using the radial receiver function. We minimize the effect of lateral heterogeneity on our result and enhance the multiples by using data with periods longer than 3–5 s.

TABLE 1 Poisson's ratio and crustal thickness by crustal type

Crustal type*	Vol. %†	No. obs‡	v_P§ (km s^{-1})	σ_{ave}	σ_{sd}	σ_m	h_{ave} (km)	h_{sd} (km)	h_m (km)
Shield	16	14 (0)	6.5	0.29	0.02	0.29	36.9	2.9	35.7
Platform	51	7 (3)	6.5	0.27	0.03	0.26	41.5	6.8	40.7
Pal.	19	17 (4)	6.5	0.27	0.03	0.27	33.4	5.6	33.4
M–C	14	24 (2)	6.25	0.25	0.04	0.24	32.6	6.8	31.1
IA	—	4 (1)	6.75	0.31	0.05	0.33	28.5	3.6	27.6

σ, Poisson's ratio; *h*, crustal thickness.
* Defined in Fig. 2 legend.
† Normalized continental crustal volume percentage calculated from surface area percentage[16] and our estimated average crustal thicknesses.
‡ Number of measurements used to calculate average (subscript ave), standard deviation (sd), and median (m). Numbers in parentheses are measurements truncated from calculation because they were more than ±0.07 from the initial average.
§ Average crustal velocity used in the calculation of Poisson's ratio and crustal thickness. Estimates taken from global compilations of seismic refraction and reflection studies[29].